Thermal and Electrical Transport in Ultralow Density Single-Walled Carbon Nanotube Networks

*Ke Jia Zhang, Abhishek Yadav, Kyu Hun Kim, Youngseok Oh, Mohammad F. Islam, Ctirad Uher, and Kevin P. Pipe**

Carbon nanotube networks offer significant technological promise as a means of realizing, on a macroscopic size scale, the excellent thermal, electrical, mechanical, and functionalization properties of nanotubes, in general, and single-walled carbon nanotubes (SWCNTs), in particular. In such networks, the properties of the junctions between nanotubes can critically determine the performance of the entire network. For thermal and electrical applications of uncoated SWCNT networks, nanotube junctions are the primary bottleneck for heat and charge transfer, since thermal and electrical conductivities are high within the SWCNTs themselves.[1–3] In addition to the intrinsic impedances of the individual junctions, collective effects (e.g., phonon interference) are believed to arise due to the interconnected nature of the network and contribute to the total impedance; Green's functions calculations that include such effects have been used to study the large increases observed in junction impedance for SWCNT networks relative to that measured at the junction of two isolated (i.e., not within a network) SWCNTs.[1]

In this work, we present the temperature-dependent (100–300 K) thermal, electrical, and thermoelectric properties of SWCNT aerogels with ultralow density ($\rho \approx 6.6$ kg m^{-3}). The aerogels are three-dimensional, isotropic networks of SWCNTs held together by van der Waals interactions at the junctions between nanotubes.[4] Their ultralow density leads to an inter-junction spacing (mesh size) of 20 nm,[5] which is much larger than previous SWCNT networks (mesh size ≈ 2 nm)[1] in which these transport properties have been studied. This enables the transport properties of the junctions to be distinguished from those of the nanotubes themselves. We measure dramatic (order of magnitude) improvements in the thermal and electrical conductances of the SWCNT junctions compared with previously reported junction conductances in SWCNT networks. The average junction conductances of the aerogel network are found to be close to the ideal thermal and electrical conductances at the junction of two isolated (non-network) van der Waals bonded SWCNTs,[2,6] suggesting the possible elimination of collective effects. We find that coating the junctions and nanotubes with a few layers of graphene to improve the aerogel network's mechanical properties[4] degrades its electrical and thermal performance, as the junction impedances become outweighed by the increased impedances of the coated SWCNTs themselves. The coating further leads to a plateau in the aerogel thermal conductivity over a range of temperatures, which we show is consistent with a temperature-dependent phonon mean free path.[7]

Aerogels were synthesized from SWCNTs (SouthWest NanoTech) with length $l \approx 1$ μm and diameter $d \approx 0.93$ nm through a critical point drying technique. Two types of aerogels were considered: as-grown SWCNT samples ($\rho \approx 6.6$ kg m^{-3}) and graphitic layer coated (Gr-coated) SWCNT samples ($\rho \approx 16.1$ kg m^{-3}, synthesized from as-grown samples) that have significantly improved mechanical properties.[4] Transmission electron microscopy (Supporting Information, Figure S1) and Raman spectroscopy measurements confirmed that the latter samples were coated with between one and five layers of ≈3 nm-long graphitic nanoplates, and that the underlying SWCNTs remained intact during the coating process.[4] The graphitic coating was also observed to accumulate at the SWCNT junctions, which likely strengthened these junctions and improved their mechanical properties.[4]

Thermal conductivity was measured using a comparative method (Supporting Information, Figure S2) that is standard for materials with low thermal conductivity.[8] A disc-shaped sample of radius 10 mm and thickness 3 mm was sandwiched between two stainless-steel discs (SS304), each having a radius of 10 mm, thickness of 10 mm, and temperature-dependent thermal conductivity that was previously measured. Silver paste (DuPont 4929N) was used to reduce the contact resistance between the aerogel and steel plates, and did not permeate the samples. A heater was mounted on top of one steel plate and used to generate a heat current while the other plate was placed in contact with the cold finger of a cryostat, thereby realizing a standard heat flux measurement geometry. Measurements

K. J. Zhang, Dr. A. Yadav, Prof. K. P. Pipe
Department of Mechanical Engineering
University of Michigan
2350 Hayward, Ann Arbor, MI 48109, USA
E-mail: pipe@umich.edu
Dr. A. Yadav, Prof. C. Uher, Prof. K. P. Pipe
Center for Solar and Thermal Energy Conversion (CSTEC)
University of Michigan
2300 Hayward Street, Ann Arbor, MI 48109, USA
K. H. Kim, Dr. Y. Oh, Prof. M. F. Islam
Department of Materials Science & Engineering
Carnegie Mellon University
5000 Forbes Avenue, Pittsburgh, PA 15213, USA
Prof. C. Uher
Department of Physics
University of Michigan
450 Church Street, Ann Arbor, MI 48109, USA
Prof. K. P. Pipe
Department of Electrical Engineering and Computer Science
University of Michigan
1301 Beal Avenue, Ann Arbor, MI 48109, USA

DOI: 10.1002/adma.201300059

were conducted in vacuum to prevent parasitic convection. Two copper cylinders were mounted outside the cold finger as radiation shields. The temperature of the sample holder was controlled by a Lakeshore 340 temperature controller. Six thermocouples (TC1–TC6) were inserted into small-bore holes in the steel plates and affixed to the top and bottom of the sample and were used in separate measurements to determine: 1) the heat fluxes through the steel plates (TC5, TC6) and temperature drop across the sample (TC3, TC4) when the heater was turned on (from which the sample's thermal conductivity was derived), 2) the temperature drop and induced thermal voltage (TC3, TC4) across the sample when the heater was turned on (from which the sample's Seebeck coefficient was derived), and 3) the voltage drop across the sample (TC3, TC4) when the current source (I) was turned on (from which the sample's electrical conductivity was derived).

The sample thermal conductivity (κ) was derived using the 1D Fourier law $k = Qt_s/(A_s(T_3 - T_4))$ where t_s and A_s are the sample thickness and cross-sectional area and Q is the heat flux through the sample. Q was estimated using the heat flux $A_b k_b (T_5 - T_6)/t_b$ transferred through the bottom steel plate, where k_b is the steel plate thermal conductivity and t_b is the distance between TC5 and TC6. Three sources of error (discussed further in the Supporting Information) are associated with Q: uncertainty due to parasitic black-body radiation losses from the sample (calculated to be less than 7.4%), uncertainty due to parasitic conduction losses through the thermocouples (calculated to be less than 0.1%), and uncertainty in t_b due to the nonzero thermocouple diameter (calculated to be less than 10%). Direct calculation of the heat loss by comparison of the heat fluxes in the top and bottom steel plates, while having a larger uncertainty than the component analysis above due to the collective uncertainties associated with a larger number of thermocouples, likewise suggested that the heat loss was small compared to Q. The uncertainty in t_s due to surface roughness was approximately 5%, and the uncertainties in temperature and voltage measurements were each less than 0.01%. The interfacial temperature drops at each end of the sample were estimated to be less than 0.3% of the temperature drop across the sample itself. The fraction of Q carried by radiative heat transfer within the aerogel was calculated by photon diffusion theory[13] to be between 0.3% and 2.3% for the as-grown sample and between 0.3% and 2.7% for the Gr-coated sample over the range of 100–300 K. Accounting for the above sources of uncertainty (discussed further in the Supporting Information), the maximum error in thermal conductivity is found to be 18%. Since the same bottom steel plate was used for all measurements (thus fixing t_b), the relative uncertainty in thermal conductivity for the two aerogel samples is less than 9%.

The measured thermal conductivities of the as-grown and Gr-coated SWCNT aerogels at room temperature are shown in **Figure 1**a. Both aerogels are found to have thermal conductivities similar to conventional carbon aerogels (CAs) of much higher density.[15–17] At room temperature, the average k/ρ is 85.9 W cm^2 kg^{-1} K^{-1} for the as-grown aerogels and 14.6 W cm^2 kg^{-1} K^{-1} for the Gr-coated aerogels, both of which are much higher than that found in CAs (typically ≈5 W cm^2 kg^{-1} K^{-1}). Figures 1b,c show the temperature dependence of thermal conductivity measured for the SWCNT aerogels

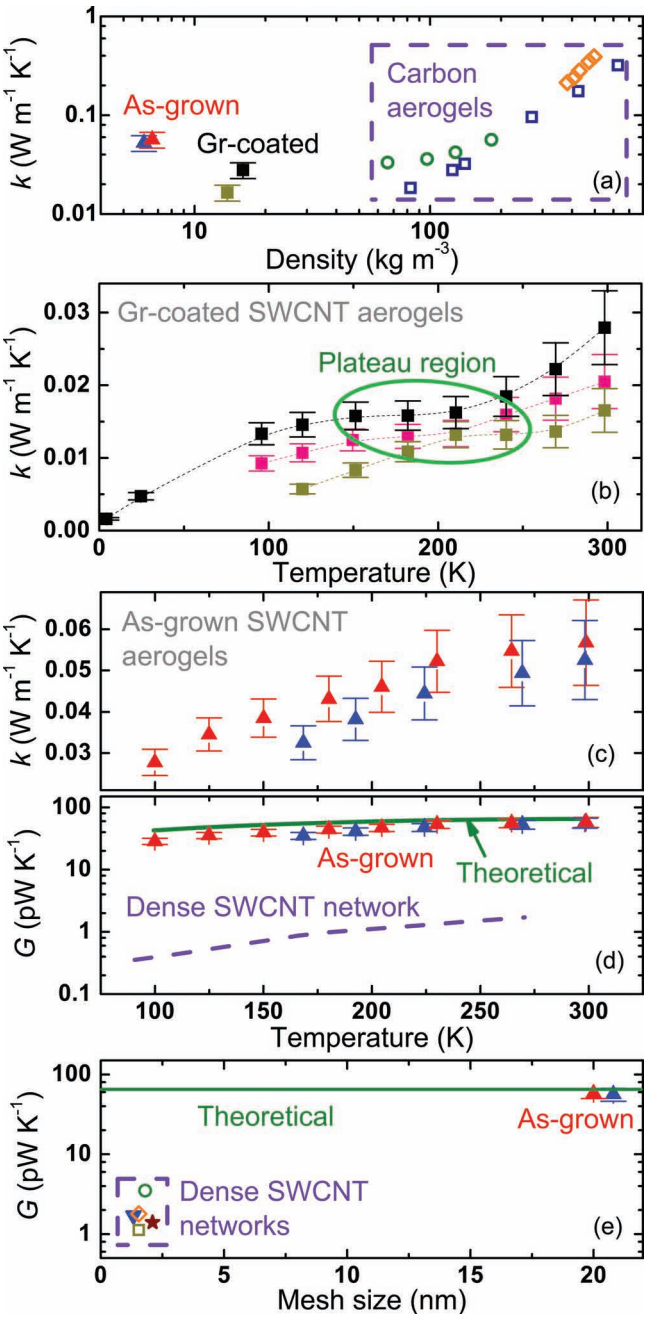

Figure 1. Thermal properties. a) Thermal conductivities of SWCNT aerogels and carbon aerogels (CAs) with various densities at room temperature. ▲ (red and blue): as-grown, ■ (black and brown): Gr-coated, □,○,◇: CAs.[15–17] b, c) Thermal conductivities of (b) Gr-coated and (c) as-grown SWCNT aerogels as a function of temperature (excluding thermal radiation within the aerogel). d) Derived average junction thermal conductances for two as-grown SWCNT aerogels (data points) and for a dense SWCNT network (dashed line),[23] as well as the theoretical junction thermal conductance of two isolated (non-network) van der Waals bonded (10,0) SWCNTs (solid line).[2] e) Average junction thermal conductances of SWCNT networks with various mesh sizes: dense networks (▼,◇, □,★)[23,27–29] and as-grown SWCNT aerogels (▲ red and blue). For ◇ and □, an isotropic SWCNT network of volume fraction 70% (typical of buckypaper)[30] was used to estimate the mesh size. Also shown is the theoretical junction thermal conductance of two isolated (non-network) van der Waals bonded (10,0) SWCNTs (dashed line)[2] and three crossed SWCNTs (○) from a Green's function calculation.[1]

primarily over the range of 100–300 K. The thermal conductivities of the as-grown aerogels strictly increase with temperature, similar to a single isolated (non-network) SWCNT-SWCNT junction over this temperature range.[2] While the Gr-coated aerogels are more than twice as dense, their thermal conductivities are approximately half that of the as-grown sample, and exhibit a plateau region. Such plateaus in thermal conductivity have been observed in amorphous materials (including aerogels) due to strong Rayleigh scattering of phonons from local variations in density or bond length, but typically occur in such materials at a much lower temperature (≈30 K).[18,19]

To analyze the thermal performance of the two types of aerogels, we first express the aerogel thermal resistance as $R = R_{NT} + R_{junc}$, where R_{NT} is due to transport within the SWCNTs and R_{junc} is due to transport at the junctions between the SWCNTs. R_{NT} is calculated by considering a structure that has the same radius, thickness, and density as the aerogel sample and which contains n_2 layers of SWCNTs (each having n_1 SWCNTs, all of diameter d and length l) that are perfectly aligned in the direction of the temperature gradient. R_{NT} is then given by $R_{SWCNT} \times n_2/n_1$, where R_{SWCNT} is the thermal resistance of a single SWCNT. Because the phonon mean free path (l_{mfp}) of an as-grown 1 nm-diameter SWCNT is larger than 750 nm for temperatures below 300 K,[20] we assume ballistic heat transfer within the SWCNTs in the as-grown aerogel and set $l_{mfp} = l$. Applying the thermal conductivity relation $k = Cvl_{mfp}/3$,[21] we express R_{SWCNT} of the as-grown aerogels as $3/(\pi d\delta C v_B)$, where $\delta = 3.35$ Å is the graphite intersheet spacing,[20] C is the SWCNT specific heat (taken to vary from 153 to 641 J kg^{-1} K^{-1} over the range of 100–300 K based on data for an isolated uncoated (10, 10) SWCNT),[22] and v_B is the ballistic phonon group velocity, which is independent of nanotube length and calculated as ≈1.5×10^7 m s^{-1} based on $v_B = 3k/(Cl_{mfp})$ and measurement data of an as-grown 1 nm-diameter SWCNT.[20] The above calculations predict a contribution of R_{NT} to the total measured SWCNT aerogel thermal resistance of only 0.3–0.8%; similar to other SWCNT networks, the resistance of the as-grown sample is therefore dominated by junction resistances.[1,23]

For a network of junctions each having thermal conductance G, the total contribution of the junctions to the aerogel thermal conductivity can be derived using an excluded volume approach.[11,24] Properly accounting for the transport properties of the 3D random SWCNT network (which yields electrical and thermal conductivities proportional to ρ^2 [3,11,24,25] rather than ρ[1,2,26]), we apply the density relation $\rho = 2\pi d\rho_{graphene}/\overline{D}^2$ [2] to the network thermal conductivity $k = Gl^2(\rho/\rho_{graphene})^2/(72\pi d)$[24] to derive the junction contribution to thermal conductivity $k_{junc} = \pi G l^2 d_t/(18\ \overline{D}^4)$ and the total junction thermal resistance $R_{junc} = 18\ \overline{D}^4 t_s/(\pi l^2 d G A_s)$. An average mesh size of $\overline{D}$ = 20 nm was used for the as-grown samples (which had volume fractions of 0.52% and 0.49%) based on small-angle neutron-scattering measurements of as-grown SWCNT aerogels with 0.5% volume fraction.[5] As shown in Figure 1d,e, the average individual junction conductances of the as-grown SWCNT aerogels derived from their measured thermal conductivities are very close to the value of 60 pW K^{-1} predicted by a Green's function model for a single isolated (non-network) van der Waals bonded SWCNT junction.[2] To compare these average individual junction conductances to those of dense SWCNT networks, we again apply the SWCNT network density relation and derive values of G for dense SWCNT networks[23,27]–[29] using $G = G_{AG}(\rho_{AG}/\rho)^2 k/k_{AG}$, where AG refers to the as-grown aerogel. Note that the thermal conductance of a single junction is proportional to k/ρ^2. The results, also plotted in Figure 1d,e, show that the thermal conductances of junctions in dense SWCNT networks have a typical magnitude of 2 pW K^{-1}, 30 times less than that of the as-grown aerogel.

Reduction of the junction thermal conductance due to phonon interference has been proposed based on atomistic Green's function simulations[1] as a reason for the very small measured thermal conductivities of dense SWCNT networks, since the phonon coherence length in SWCNTs is on the order of micrometers.[20] Based on a simple dominant phonon model[31] and a longitudinal acoustic phonon velocity of 24 km s^{-1},[22] the dominant phonon wavelength is predicted to be 1.5 nm at 300 K and 4.5 nm at 100 K. Dense SWCNT networks previously studied have a typical mesh size of 2.5 nm,[23,27–29] making the space between adjacent SWCNTs less than 1 nm. Because of their relatively wide junction spacing, interference effects are expected to be less pronounced in aerogel networks; this is supported by the similarity of the derived average as-grown junction conductance to the predicted value for a single isolated (non-network) SWCNT junction. Furthermore, since ultralow density SWCNT networks exhibit the intrinsic properties of SWCNT-SWCNT junctions, they provide an accurate means to characterize single-junction thermal properties that is much simpler and less prone to significant experimental uncertainties than measuring a single-junction resistance directly.[32]

The graphitic layers (composed of ≈3 nm long flakes between 1 and 5 atomic layers thick)[4] accumulated at the junctions of the Gr-coated aerogel are expected to increase the contact area of each junction and hence its conductance G.[32,33] Using the average number of layers (2.5) to scale[32] the junction conductance of the Gr-coated sample relative to that of the as-grown sample through $G_{Gr} = G_{AG}(d_{Gr}/d_{AG})^2$, and accounting for its same average mesh size $\overline{D}$ = 20 nm (since the graphitic coating is applied to the as-grown sample and therefore does not affect the mesh size[4]), we plot the calculated total junction resistance R_{junc} as well as the total measured thermal resistance R in **Figure 2**a. The junction resistance is found to have only a small (less than 8%) contribution in these samples which is not large enough to account for the measured thermal conductivity plateau.

To analyze this plateau, we take the difference $R - R_{junc}$ to be the resistance of the Gr-coated SWCNTs themselves (R_{NT}) and study the effect of the graphitic layers on phonon boundary scattering. Using the same ballistic phonon velocity as derived for the as-grown aerogel, we find that l_{mfp} for the Gr-coated SWCNT aerogel is on the same order as the nanotube diameter, consistent with the Casimir limit ($l_{mfp} \approx d$)[34] and other 1D nanostructures such as Si nanowires coated with germanium.[35] Previous models for coated 1D systems have predicted a frequency-dependent l_{mfp} that falls to a minimum at a particular frequency due to strong phonon coupling at that frequency between the 1D system and coating.[7] Using a dominant phonon model[31] and the Debye temperature T_D = 960 K for (10, 10) SWCNTs,[22] we translate this frequency

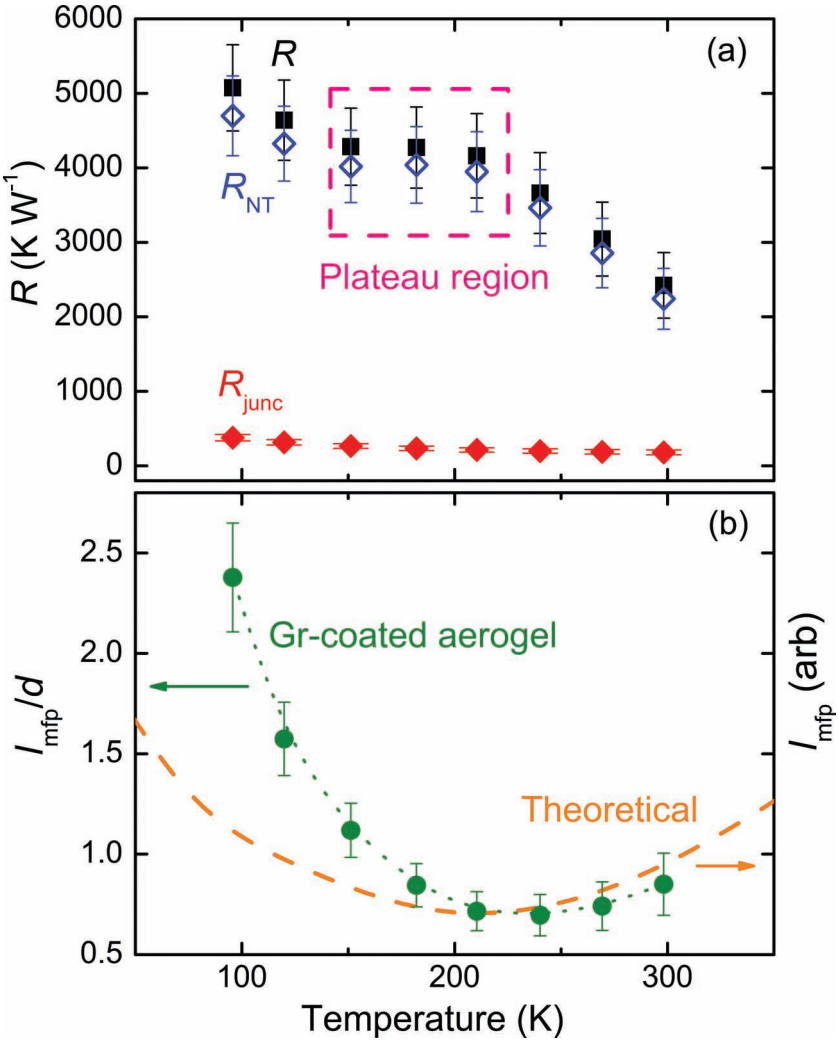

Figure 2. Analysis of observed thermal conductivity plateau. a) Temperature-dependent components of thermal resistance for Gr-coated aerogel. ■: R from measurement (radiation excluded), ◇: R_{NT}, ✦: R_{junc}. b) Temperature-dependent phonon mean free path l_{mfp}: predicted for a coated nanowire (orange dashed line),[7] derived for Gr-coated SWCNT aerogel (●).

dependence into a temperature dependence, finding qualitative agreement with the trend in $l_{mfp}(T)$ derived for the Gr-coated samples (Figure 2b) and quantitative agreement in the temperature of the minimum. This analysis suggests that the thermal conductivity plateau observed for the Gr-coated aerogel is due to the dominant phonon mean free path reaching a minimum at that temperature.

Measured electrical conductivities of the SWCNT aerogels (derived from $\sigma = It/(VA_s)$, where V is the voltage drop measured across the sample when current I is applied) are shown in **Figure 3**a. As observed in other SWCNT networks, the electrical conductivities of all samples increase with temperature, presumably due to tunneling at the junctions.[23] Like the thermal conductivity measurements, the electrical conductivities of the Gr-coated samples are found to be much lower than that of the as-grown sample.

Similar to phonon transport, the mean free path and coherence length of electrons in SWCNTs are generally assumed to be on the order of micrometers,[36] making electrical transport in uncoated SWCNT networks also dominated by transport at the junctions.[3] In the same way that the average junction thermal conductance in a network is proportional to k/ρ^2, the average junction electrical conductance in a network is proportional to σ/ρ^2. As shown in Figure 3d, the average junction electrical conductance of an as-grown SWCNT aerogel is approximately 2 orders of magnitude greater than that of a dense or bundled SWCNT network.[23,25] Following calculations equivalent to those given above for thermal conductance, we derive an average junction contact resistance for the as-grown aerogel of 9.8 MΩ. While smaller values in the range of 0.43–2.3 MΩ have been measured for a junction between two isolated (non-network) SWCNTs on a silicon dioxide substrate,[6] it has been shown that substrate effects can pull SWCNTs into closer contact than when they are free-standing as in the SWCNT aerogels measured here.[6] The similarity in the temperature dependences of the electrical conductance for the SWCNT aerogel junctions and the isolated (non-network) junction (Figure 3b) further supports the electrical ideality of the SWCNT aerogel junctions.[37]

The Gr-coated aerogel has a lower electrical conductivity than the as-grown aerogel (suggesting increased carrier scattering due to the coating) and greater temperature dependence (Figure 3c) than the as-grown aerogel, a single SWCNT, single-layer graphene, bilayer graphene, or a graphene ribbon.[38–40] These differences between the as-grown and Gr-coated aerogels likely arise from a perturbation of the structural symmetry and band structure of the SWCNTs by the graphitic coating, similar to the way in which these characteristics are perturbed in single-layer graphene when a second layer is added.[39] The derived activation energy for the Gr-coated aerogel is E_a = 34 meV, similar to values found for graphene ribbons.[40]

Measured thermopower (Seebeck coefficient, S) data for the SWCNT aerogels are shown in Figure S3 in the Supporting Information. Unlike thermal conductivity and electrical conductivity, thermopower does not have a strong dependence on density. The similarity of the thermopower of the as-grown aerogel to that of a single (10, 0) SWCNT[20] or a dense SWCNT network[41] suggests that it is not strongly dependent on junction properties. Both experiments[20] and simulations[42] have suggested that phonon drag effects can strongly contribute to the thermopower of a SWCNT and can increase over the temperature range of 10 K to 300 K. The thermopower is found to be much lower for the Gr-coated aerogel than the as-grown aerogel, as increased phonon boundary scattering reduces ballistic phonon transport and hence the contribution of phonon drag (as well as the thermal conductivity, as discussed above).

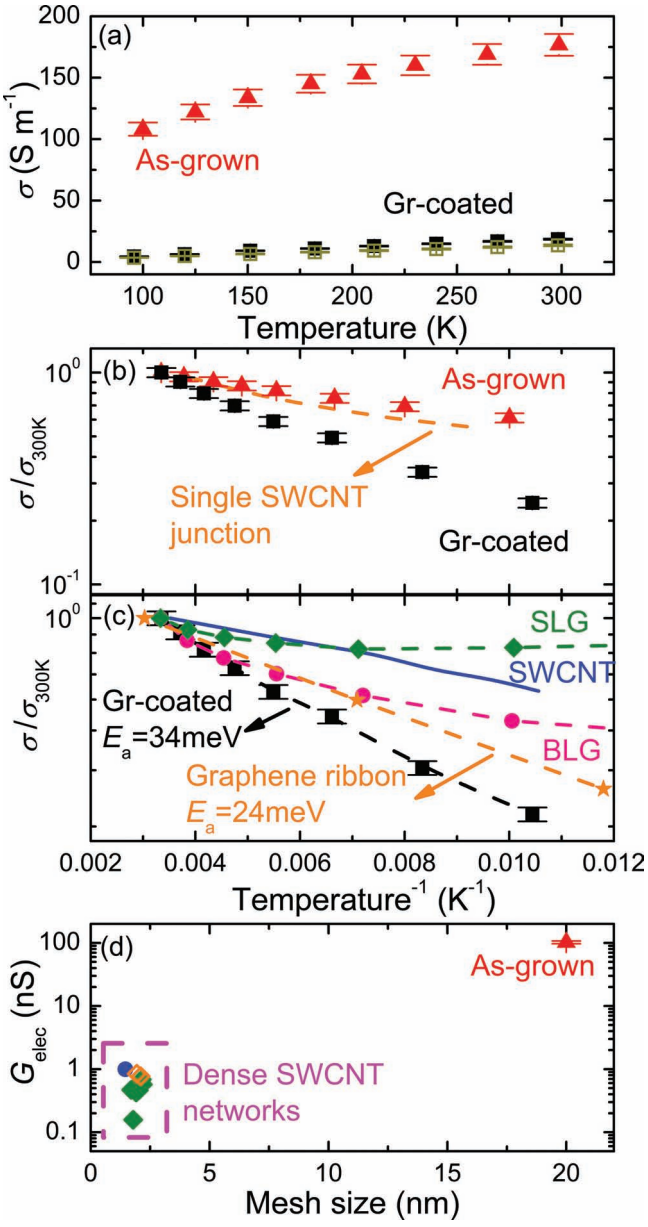

Figure 3. Electrical properties. a) Electrical conductivities of SWCNT aerogels vs. temperature. ▲: as-grown, ■(black and olive): Gr-coated. b) Temperature dependence of normalized conductivity of SWCNT aerogels. Data for an isolated (non-network) junction between two metallic SWCNTs is shown as a dashed line.[37] c) Temperature-dependent normalized conductivity of Gr-coated aerogel and: (solid line) single 1.3 nm diameter SWCNT;[38] ✦: single layer of graphene;[39] ●: bilayer graphene;[39] ✦: 36 nm wide graphene ribbon.[40] d) Junction electrical conductances of as-grown aerogel and dense SWCNT networks at room temperature. ◇,✦, ●: dense networks.[25,25,23]

In conclusion, measurements of the thermal, electrical, and thermoelectric properties of ultralow density SWCNT aerogels over the range of 100–300 K indicate that the thermal and electrical conductances of the constituent junctions are much higher than those found in dense SWCNT networks and approach the ideal values of isolated (non-network) SWCNT junctions. In particular, the junction thermal conductance of the as-grown aerogel is very close to the theoretical maximum for a van der Waals bonded SWCNT junction. Graphitic coatings used to improve the aerogel mechanical strength are found to greatly inhibit thermal and electrical transport. Reduction in phonon mean free path is evidenced by both thermal conductivity and thermopower measurements; the latter suggests that increased phonon boundary scattering in the Gr-coated aerogel reduces the contribution of phonon drag.

Supporting Information

Supporting Information is available from the Wiley Online Library or from the author.

Acknowledgements

K.J.Z., A.Y., K.H. K.,Y.O., M.F.I., and K.P.P. acknowledge the National Science Foundation (NSF) for its support of sample preparation and measurement through Grant No. CBET-0933510. K.H.K., Y.O., and M.F.I. acknowledge the support of NSF for sample synthesis methods through Grant No. DMR-0645596. C.U. acknowledges support for sample measurement as part of the Center for Solar and Thermal Energy Conversion, an Energy Frontier Research Center funded by the U.S. Department of Energy, Office of Science, Basic Energy Sciences under Award No. DE-SC0000957.

Received: January 4, 2013
Revised: March 4, 2013
Published online: April 22, 2013

[1] R. S. Prasher, X. J. Hu, Y. Chalopin, N. Mingo, K. Lofgree, S. Volz, F. Cleri, P. Keblinski, *Phys. Rev. Lett.* **2009**, *102*, 105901.
[2] Y. Chalopin, S. Volz, N. Mingo, *J. Appl. Phys.* **2009**, *105*, 084301.
[3] P. N. Nirmalraj, P. E. Lyons, S. De, J. N. Coleman, J. J. Boland, *Nano. Lett.* **2009**, *9*, 3890.
[4] a) K. H. Kim, Y. Oh, M. F. Islam, *Nat. Nanotechnol.* **2012**, *7*, 562; b) K. H. Kim, Y. Oh, M. F. Islam, *Adv. Funct. Mater.* **2013**, *23*, 377.
[5] L. A. Hough, M. F. Islam, B. Hammouda, A. G. Yodh, P. A. Heiney, *Nano. Lett.* **2006**, *6*, 313.
[6] M. S. Fuhrer, J. Nygard, L. Shih, M. Forero, Y. G. Yoon, M. S. C. Mazzoni, H. J. Choi, J. Ihm, S. G. Louie, A. Zettl, P. L. McEuen, *Science* **2000**, *288*, 494.
[7] N. Mingo, L. Yang, *Phys. Rev. B.* **2003**, *68*, 245406.
[8] J. Hone, M. Whitney, C. Piskoti, A. Zettl, *Phys. Rev. B.* **1999**, *59*, R2514.
[9] R. Fainchtein, D. M. Brown, K. M. Siegrist, A. H. Monica, E. Hwang, S. D. Milner, C. C. Davis, *Phys. Rev. B.* **2012**, *85*, 125432.
[10] M. A. Panzer, H. M. Duong, J. Okawa, J. Shiomi, B. L. Wardle, S. Maruyama, K. E. Goodson, *Nano Lett.* **2010**, *10*, 2395.
[11] A. N. Volkov, L. V. Zhigilei, *Phys. Rev. Lett.* **2010**, *104*, 215902.
[12] Z. P. Yang, L. Ci, J. A. Bur, S. Y. Lin, P. M. Ajayan, *Nano Lett.* **2008**, *8*, 446.
[13] H. P. Ebert, in *Aerogels Handbook*, *1st ed.*, (Eds: M. A. Aegerter, N. Leventis, M. M. Koebel), Springer, New York **2011**, Ch. 23.
[14] M. Wiener, G. Reichenauer, S. Braxmeier, F. Hemberger, H. P. Ebert, *Int. J. Thermophys.* **2009**, *30*, 1372.
[15] X. Lu, O. Nilsson, J. Fricke, R. W. Pekala, *J. Appl. Phys.* **1993**, *73*, 581.
[16] J. Feng, J. Feng, C. Zhang, *J. Porous Mater.* **2012**, *19*, 551.
[17] V. Bock, O. Nilsson, J. Blumm, J. Fricke, *J. Non-cryst. Solids.* **1995**, *185*, 233.
[18] A. Jagannathan, R. Orbach, O. E. Wohlman, *Phys. Rev. B.* **1989**, *39*, 13465.

[19] J. E. Graebner, B. Golding, L. C. Allen, *Phys. Rev. B.* **1986**, *34*, 5696.
[20] C. Yu, L. Shi, Z. Yao, D. Li, A. Majumda, *Nano Lett.* **2005**, *5*, 1842.
[21] C. Kittel, *Introduction to Solid State Physics*, *7th ed.*, John Wiley and Sons, New York **1996**, Ch. 5.
[22] J. Hone, in *Carbon Nanotubes: Synthesis, Structure, Properties and Applications*, *Topics in Applied Physics, Vol. 80* (Eds: M. S. Dresselhaus, G. Dresselhaus, P. Avouris), Springer-Verlag, Berlin Heidelberg **2001**, Ch. 11.
[23] M. E. Itkis, F. Borondics, A. Yu, R. C. Haddon, *Nano Lett.* **2007**, *7*, 900.
[24] Y. Chalopin, S. Volz, N. Mingo, *J. Appl. Phys.* **2010**, *108*, 039902.
[25] P. E. Lyons, S. De, F. Blighe, V. Nicolosi, LFC. C. Pereira, M. S. Ferreira, J. N. Coleman, *J. Appl. Phys.* **2008**, *104*, 044302.
[26] S. N. Schiffres, K. H. Kim, L. Hu, A. J. H. McGaughey, M. F. Islam, J. A. Malen, *Adv. Funct. Mater.* **2012**, *22*, 5251.
[27] J. Hone, M. C. Llaguno, N. M. Nemes, A. T. Johnson, J. E. Fischer, D. A. Walters, M. J. Casavant, J. Schmidt, R. E. Smalley, *Appl. Phys. Lett.* **2000**, *77*, 666.
[28] P. Gonnet, Z. Liang, E. S. Choi, R. S. Kadambala, C. Zhang, J. S. Brooks, B. Wang, L. Kramer, *Curr. Appl. Phys.* **2006**, *6*, 119.
[29] J. E. Fischer, W. Zhou, J. Vavro, M. C. Llaguno, C. Guthy, R. Haggenmueller, M. J. Casavant, D. E. Walters, R. E. Smalley, *J. Appl. Phys.* **2003**, *93*, 2157.
[30] B. W. Simth, Z. Benes, D. E. Luzzi, J. E. Fischer, D. A. Walters, M. J. Casavant, J. Schmidt, R. E. Smalley, *Appl. Phys. Lett.* **2000**, *77*, 663.
[31] R. Prasher, T. Tong, A. Majumdar, *Nano Lett.* **2008**, *8*, 99.
[32] J. Yang, S. Waltermine, Y. Chen, A. A. Zinn, T. T. Xu, D. Li, *Appl. Phys. Lett.* **2010**, *96*, 023109.
[33] W. J. Evans, M. Shen, P. Keblinski, *Appl. Phys. Lett.* **2012**, *100*, 261908.
[34] Y. F. Zhu, J. S. Lian, Q. Jiang, *Appl. Phys. Lett.* **2008**, *92*, 113101.
[35] R. Yang, G. Chen, *Nano Lett.* **2005**, *5*, 1111.
[36] M. S. Purewal, B. H. Hong, A. Ravi, B. Chandra, J. Hone, P. Kim, *Phys. Rev. Lett.* **2007**, *98*, 186808.
[37] J. W. Park, J. Kim, K. H. Yoo, *J. Appl. Phys.* **2003**, *93*, 4191.
[38] C. Zhou, J. Kong, H. Dai, *Phys. Rev. Lett.* **2000**, *84*, 5604.
[39] S. V. Morozov, K. S. Novoselov, M. I. Katsnelson, F. Schedin, D. C. Elias, J. A. Jaszczak, A. K. Geim, *Phys. Rev. Lett.* **2008**, *100*, 016602.
[40] M. Y. Han, J. C. Brant, P. Kim, *Phys. Rev. Lett.* **2010**, *104*, 056801.
[41] L. Grigorian, K. A. Williams, S. Fang, G. U. Sumanasekera, A. L. Loper, E. C. Dickey, S. J. Pennycook, P. C. Eklund, *Phys. Rev. Lett.* **1998**, *80*, 5560.
[42] M. Tsaousidou, *Phys. Rev. B.* **2010**, *81*, 235425.